Am J Transl Res 2015;7(1):79-87
www.ajtr.org /ISSN:1943-8141/AJTR0003141

Original Article

Visualization of *in vivo* thromboprophylactic and thrombolytic efficacy of enoxaparin in laser-induced vascular endothelial injury model using multiphoton microscopy

Koji Tanaka[1], Yuhki Koike[1], Kohei Matsushita[1], Masato Okigami[1], Yuji Toiyama[1], Mikio Kawamura[1], Susumu Saigusa[1], Yoshinaga Okugawa[1], Yasuhiro Inoue[1], Keiichi Uchida[1], Toshimitsu Araki[1], Yasuhiko Mohri[1], Akira Mizoguchi[2], Masato Kusunoki[1]

Departments of [1]Gastrointestinal and Paediatric Surgery, [2]Neural Regeneration and Cell Communication, Mie University Graduate School of Medicine, 2-174 Edobashi, Tsu, Mie 514-8507, Japan

Received October 14, 2014; Accepted November 25, 2014; Epub January 15, 2015; Published January 30, 2015

Abstract: Enoxaparin is used postoperatively for the prevention of venous thromboembolism. *In vitro* studies and clinical trials have demonstrated the anticoagulant and antithrombotic efficacy of enoxaparin. In this study, we visualised thromboprophylactic and thrombolytic efficacy of enoxaparin in a laser-induced thrombus formation model *in vivo* using two-photon laser-scanning microscopy (TPLSM). Thrombus was induced by the selective irradiation of vascular endothelium in arterioles of the cecum of green fluorescent protein transgenic mice. The thromboprophylactic and thrombolytic efficacy of enoxaparin was visualised *in vivo* real-time using TPLSM. Platelet adhesion, aggregation, and platelet-dependent thrombus formation were observed in the laser-induced thrombus formation model with reproducibility. Laser-induced thrombus formation was significantly inhibited by enoxaparin pretreatment as the thromboprophylactic agent, as compared with control. The mean thrombus volumes were 652 microcubic meters in mice pretreated with enoxaparin and 8906 microcubic meter in control mice. Enoxaparin reduced the volume of laser-induced thrombus when using it as a thrombolytic agent. The mean rate of reduction was 59 percent. In a lipopolysaccharide-induced sepsis model, thromboprophylactic efficacy of enoxaparin was also observed *in vivo* in real-time. *In vivo* thromboprophylactic and thrombolytic efficacy of enoxaparin can be visualised at the single platelet level in the laser-induced endothelium injury model using TPLSM.

Keywords: Enoxaparin, thrombus formation, intravital imaging, multiphoton microscopy

Introduction

Venous thromboembolism (VTE), which manifests as deep-vein thrombosis or pulmonary embolism, is a common complication of cancer [1]. Cancer patients undergoing general surgery have at least twice the risk of postoperative deep-vein thrombosis and more than three times the risk of fatal pulmonary embolism [2]. The American College of Chest Physicians guidelines recommend anticoagulant thromboprophylaxis with low molecular weight heparin (LMWH) for higher-risk general surgery patients undergoing a major procedure for cancer.

Enoxaparin is one of the LMWHs that binds to and increases the activity of antithrombin III. Enoxaparin exhibits a more favourable pharmacological side effect profile compared with unfractionated heparin. Clinical trials have demonstrated the anticoagulant and antithrombotic efficacy of enoxaparin for VTE prophylaxis in cancer patients undergoing abdominal and pelvic surgery [3-5]. Therefore, enoxaparin is still the most widely used drug in the management of VTE with substantial efficacy and safety.

In vitro studies have greatly advanced our understanding of the molecular bases of haemostasis and thrombosis by identifying enzymes, cofactors, cell receptors, and associated ligands related to the haemostatic process and its regulation [6-8]. Despite these great advances, *in vivo* knowledge of comprehensive interactions by all components related to the haemo-

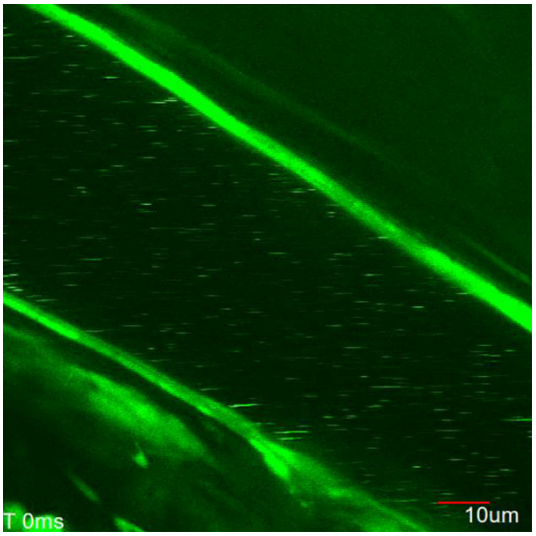

Figure 1. *In vivo* real-time imaging of blood flow in arterioles of murine cecum. Within the vessels of GFP mice, leukocytes were recognised as large, round cells and platelets were recognised as small cells. When blood flow of the arterioles was normal, leukocytes or platelets seldom adhered to the endothelium (Supplementary movie 1).

static and thrombotic processes has been limited.

Two-photon laser-scanning microscopy (TPLSM) has revolutionised *in vivo* real-time imaging with the benefits of higher resolution, increased tissue penetration, and less photodamage (or photobleaching). We previously reported a method of *in vivo* real-time imaging of laser-induced thrombus formation using TPLSM with an organ stabilising system, which allows high magnification (×600 or higher) and high resolution (at the single platelet level) images in living animals [9-15].

To reproduce the molecular bases of haemostasis and thrombosis *in vitro*, we observed the thromboprophylactic and thrombolytic effect of enoxaparin on platelet-dependent thrombus formation by laser-induced endothelium specific injury using green fluorescent protein (GFP) transgenic mice. We also observed the thromboprophylactic effect of enoxaparin in a lipopolysaccharide (LPS)-induced sepsis model.

Materials and methods

Ethics statement

This study was reviewed and approved by the Institutional Review Board and the Local Ethics Committee of the Mie University Graduate School of Medicine (No. 24-26). Written informed consent was obtained from all the patients (adults) enrolled onto the study.

The experimental protocols of in vivo studies were reviewed and approved by the Animal Care and Use Committee at the Mie University Graduate School of Medicine.

Mice

Enhanced green fluorescent protein (EGFP)-transgenic C57/BL6-Tg (CAG-EGFP) mice were purchased from Japan SLC Inc. (Shizuoka, Japan). Ten to 12-week-old male GFP mice (20–22 g) were bred, housed in groups of six mice per cage, and fed with a pelleted basal diet (CE-7; CLEA Japan Inc., Tokyo, Japan), and had free access to drinking water. Mice were kept in the animal house facilities at Mie University School of Medicine under standard conditions of humidity (50% ± 10%), temperature (23 ± 2°C) and light (12/12-h light/dark cycle), according to the Institutional Animal Care Guidelines. The experimental protocols were reviewed and approved by the Animal Care and Use Committee at the Mie University Graduate School of Medicine.

Enoxaparin

Enoxaparin sodium was purchased from Kaken Pharmaceutical Co., Ltd. (Tokyo, Japan). The stock solution was made by dissolving it in appropriate concentrations with distilled water for the *in vivo* study.

LPS

LPS (E. coli, serotype 0111:B4) was purchased from Sigma-Aldrich Co, LLC. (St Louis, MO, USA). The stock solution was made by dissolving it in appropriate concentrations with distilled water for the *in vivo* study.

Femoral venous catheterisation

To administer the accurate dose of enoxaparin reliably, a catheter (M-FAC/FVC, Neuroscience, Tokyo, Japan) was placed in the right femoral vein of anaesthetised GFP mice under surgical microscopy.

Organ stabilization for intravital imaging

After femoral venous catheterisation, GFP mice were anaesthetised using an anaesthetic mask

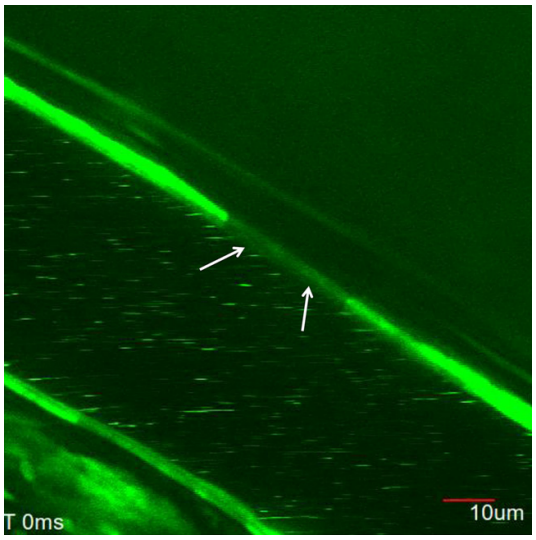

Figure 2. Platelet-dependent thrombus formation by laser-induced endothelium injury. Intravital TPLSM with an organ stabilising system provides clear visualisation of the vascular wall layer at higher magnification and higher resolution. The sophisticated and reproducible laser irradiation of the vascular endothelium (arrows) can be performed under clear and almost static visualisation of the vascular layers (Supplementary movie 2).

with 4 L/min of isoflurane (4%; Forane, Abbott, Japan). Anaesthetic maintenance was achieved using 1.5%-2% isoflurane and 4 L/min of O^2. Body temperature was kept at 37°C throughout the experiments using a heating pad. Normal saline (200 μL) was administered at 1-2-h intervals for hydration during anaesthesia through laparotomy. Lower midline laparotomy was made as short as possible (< 15 mm). The cecum and terminal ileum were identified through laparotomy. After exteriorisation of the cecum, air was introduced through the tip of the collapsed cecum using a syringe with a small needle. Optimal inflation of the cecum enabled us to visualise vertically all layers of the cecum by observing it through the serosa into the mucosa (serosal-approaching technique). The cecum was placed on wet gauze and kept moist during the experiments. The inflated cecum was put onto an organ stabilising system using a solder lug terminal with an instant adhesive agent (K0-10-p20, DAISO, Japan). This organ stabiliser minimised the microvibration of the observed area caused by heart beats and respiratory movements. Stabilisation and fixation of the cecum represented a critical but technically difficult part of the intravital TPLSM procedure. After the application of PBS to the observed area, a thin cover glass was placed gently on the cecum surface.

TPLSM setup

The procedures for TPLSM setup were performed as previously described [10]. Experiments were performed using an upright microscope (BX61WI; Olympus, Tokyo, Japan) and a FV1000-2P laser-scanning microscope system (FLUOVIEW FV1000MPE, Olympus, Tokyo, Japan). The use of special stage risers enabled the unit to have an exceptionally wide working distance. This permitted the stereotactically immobilised mouse to be placed on the microscope stage. The microscope was fitted with several lenses with high numeric apertures to provide the long working distances required for *in vivo* work, and with water-immersion optics. The excitation source in TPLSM mode was Mai Tai Ti: sapphire lasers (Spectra Physics, Mountain View, CA, USA), tuned and mode-locked at 910 nm. The Mai Tai produces light pulses of approximately 100 fs width (repetition rate of 80 MHz). Laser light reached the sample through the microscope objectives, connected to an upright microscope (BX61WI; Olympus, Tokyo, Japan). The mean laser power at the sample was between 10 and 40 mW, depending on the depth of imaging. Microscope objective lenses used in this study were the 4×UPlanSApo (numerical aperture of 0.16), the 10×UPlanSApo (numerical aperture of 0.4), and the 60×LUMPlanFI/IR (water dipping, numerical aperture of 0.9, working distance 2 mm). Data were analysed using the FV10-ASW (Olympus). TPLSM images were acquired with 512×512 pixels of spatial resolution, from a 210 μm field of view dimension, using a pixel dwelling time of 4 μs. Two-photon fluorescence signals were collected by an internal detector (non-descanned detection method) at an excitation wavelength.

Imaging methods using TPLSM

The surface of the cecum was initially screened at lower magnifications by setting out the X/Y plane and adjusting the Z axis manually to detect the optimal observation area. Each area of interest was subsequently scanned at a higher magnification (water-immersion objective 60× with or without 2× zoom) by manually setting the X/Y plane and adjusting the Z axis (either automatically or manually) to obtain

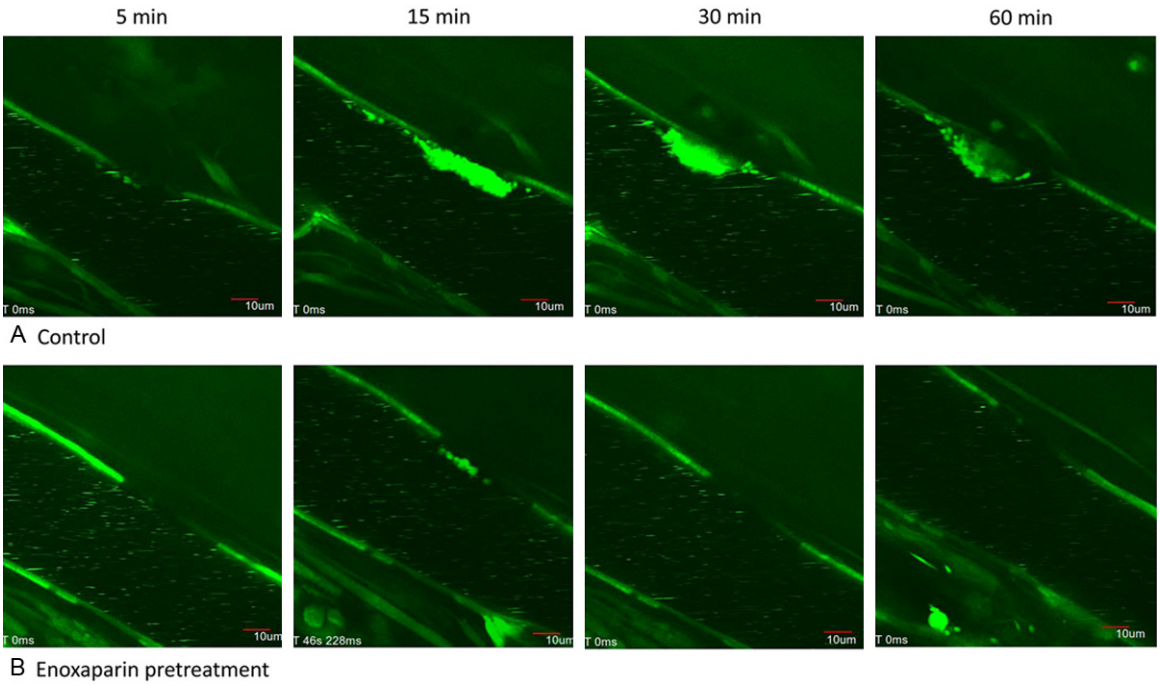

Figure 3. The time course of the thromboprophylactic effect of enoxaparin in the laser-induced thrombus model *in vivo*. The upper panel indicates the time course of laser-induced thrombus formation (control), while the lower panel indicates the time course of the thromboprophylactic efficacy of enoxaparin for laser-induced endothelium injury (enoxaparin pretreatment) *in vivo*. Supplementary movies are also available for controls at 5 min (Supplementary movie 3) and 60 min (Supplementary movie 4), and enoxaparin pretreatment at 5 min (Supplementary movie 5) and 60 min (Supplementary movie 6).

high-resolution, clear TPLSM images. The scanning areas were 200×200 μm (600×) or 100×100 μm (600× with 2× zoom). The imaging depth or imaging stack was determined arbitrarily to allow real-time three-dimensional visualisation *in vivo*. The laser power was adjusted according to the imaging depth. When imaging at larger depths, we increased the laser power level (up to 100%) manually using the laser power level controller.

In vivo thrombus formation by laser-induced vascular endothelium specific injury

The vessels in the mesentery or cremaster are commonly used in laser-induced thrombosis models because these vessels are present in two thin membranous tissues, which permit sufficient light transmission for intravital microscopy experiments. Tissue microcirculation disorders affect a number of gastrointestinal diseases. We used the arterioles of the cecum of GFP mice for *in vivo* laser-induced thrombus formation because the primary interest of our research is the pathophysiology of intestinal microcirculation disorders.

Our organ stabilising technique enables imaging of tissue microvasculature at high magnification (×600 or higher) and high resolution (at the single platelet level) *in vivo* in real-time using TPLSM. By using our system, we can perform laser irradiation for the vascular endothelial layer of cecal arterioles selectively and reproducibly under *in vivo* real-time imaging of the cecal arterioles at high magnification and high resolution [10].

Laser-induced thrombus was formed in serosal arterioles of the cecum of 30 to 100 μm in diameter according to the method of Nishimura et al [16]. The vascular endothelium was visualised and identified as a thin layer of the luminal surface of the top of the vessel, which is different from vascular smooth muscle. Laser irradiation at the two-photon wavelength of 910 nm (a Mai Tai Ti:sapphire laser light applied through a ×60 water-immersion microscope objective) was performed for the selected endothelial region for 15 to 40 sec. Laser pulses (910 nm; joules, maximum up to 192 mW) were delivered along the transverse axis of the target endothelium (via the 60× microscope objective with

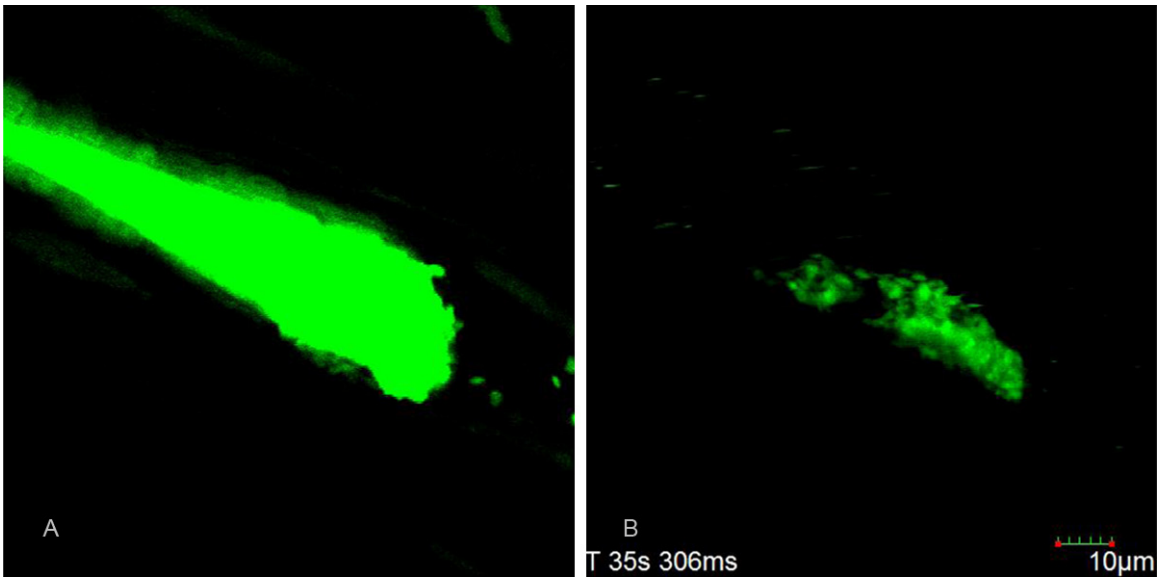

Figure 4. Thrombolytic effect of enoxaparin in the laser-induced thrombus model *in vivo*. The left panel (A) indicates an almost complete obstruction 60 min after laser-induced thrombus formation, resulting in a near complete cessation of blood flow. Supplementary movie 7 shows a process of thrombus development with the adhesion of rolling platelets on the surface of the growing thrombus. The right panel (B) shows *in vivo* thrombolytic efficacy of enoxaparin for laser-induced thrombus. Supplementary movie 8 shows a process of thrombolysis with the release of aggregated platelets on the surface of the thrombus at the single platelet level.

10× optical and digital zoom). Irradiation intensity (W/cm^2) was set depending on the vessel diameter. After identification of photobleaching of vascular endothelium, the laser power was reduced for *in vivo* imaging of thrombus formation to avoid additional photobleaching, extravasation, and undesirable vessel rupture.

The sophisticated and selective irradiation of the endothelial layer by using digital zoom (total magnification was approximately ×3000-6000) enabled reduction of undesirable target tissue damage [17].

In vivo thromboprophylactic effect of enoxaparin

Enoxaparin at a dose of 1 mg/kg or PBS (the same volume as enoxaparin) was administered intravenously via the femoral venous catheter. Thirty minutes later, laser-induced endothelium injury was achieved for real-time imaging of the thromboprophylactic effect of enoxaparin. Thrombus formation was imaged in both enoxaparin-pretreated mice and control mice.

We also imaged the thromboprophylactic effect of enoxaparin under the LPS-induced sepsis model *in vivo*.

In vivo thrombolytic effect of enoxaparin

Laser-induced thrombus was performed by irradiating endothelia of the cecal arterioles. One hour later, platelet-dependent thrombus formation was observed. Enoxaparin at a dose of 1 mg/kg or 5 mg/kg was then administered intravenously via the femoral venous catheter for real-time imaging of its thrombolytic effect.

Results

In vivo real-time imaging of blood flow in arterioles of murine cecum

Within the vessels of GFP mice, leukocytes were recognised as large, round cells and platelets were recognised as small cells. In contrast, erythrocytes were not identified [18]. Under normal blood flow of the arterioles, leukocytes or platelets seldom adhered to the endothelium (**Figure 1** and Supplementary movie 1).

Platelet-dependent thrombus formation by laser-induced endothelium injury

The endothelium of cecal arterioles was identified and then injured by a laser of 192-mW of power for 15-40 sec at 900 nm as mentioned above (Materials and Methods).

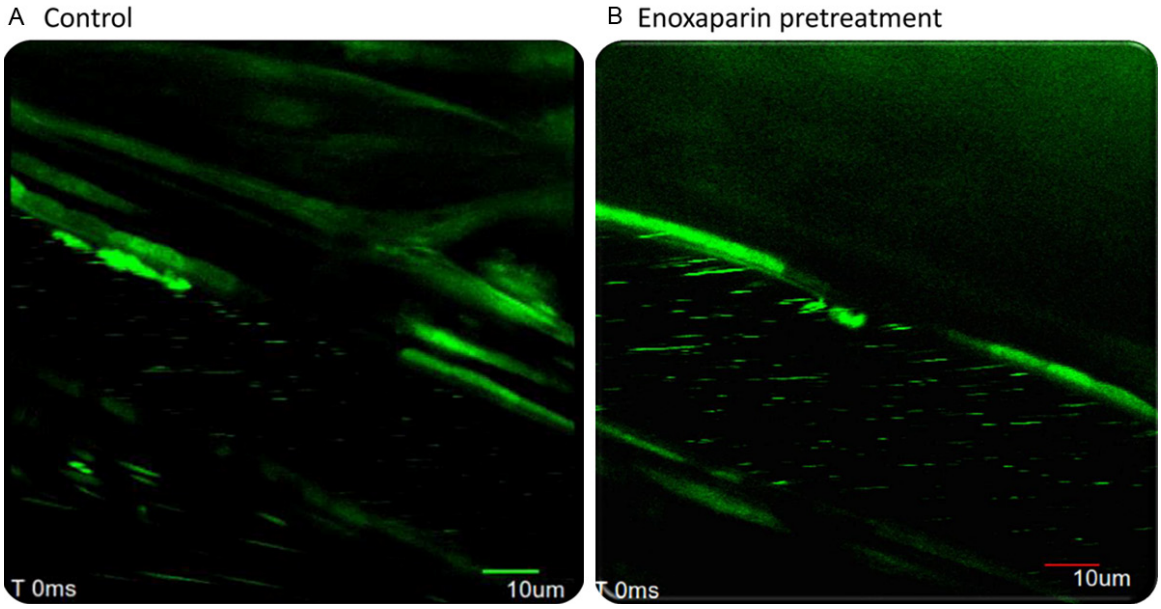

Figure 5. Thromboprophylactic efficacy of enoxaparin in the LPS-induced sepsis model *in vivo.* In LPS-administered mice, the time to maximum thrombus volume after laser irradiation was approximately half that in control mice. The left panel (A) indicates laser-induced thrombus formation in LPS-administered mice (Supplementary movie 9). The right panel (B) indicates the thromboprophylactic efficacy of enoxaparin for laser-induced thrombus formation in LPS-administered mice *in vivo* (Supplementary movie 10).

After irradiation, photobleaching was observed on the luminal surface of the top of the vessel wall (**Figure 2** and Supplementary movie 2). The mean length of such photobleaching was 20.7 ± 1.78 μm (mean ± standard deviation). There was no significant difference in the length of photobleaching between enoxaparin-pretreated mice and control mice, suggesting an achievement of a similar degree of laser-induced endothelium injury for each mouse.

The dynamic process of laser-induced thrombus formation has been described previously [10]. In brief, individual platelets were translocated on the surface of the laser-injured endothelium. Platelets then attached and adhered to the endothelium downstream of the laser-injured region. Gradually, they adhered to the laser-injured endothelium in a linear fashion (straight line formation). Circulating platelets adhered to the surface of the linear platelet adhesion. Platelet-dependent thrombus was formed forward to the upstream of the laser-injured endothelium with cycles of attachment and detachment of platelet aggregates. The thrombus developed in size with the adhesion of rolling platelets on the surface of the growing thrombus.

Approximately 60 min after laser-induced endothelial injury, platelet-dependent thrombus was formed, with a mean size of 8906 ± 1469 μm^3 (n=5 arterioles from three mice).

Thromboprophylactic effect of enoxaparin in the laser-induced thrombus model in vivo

Initially, enoxaparin at a dose of 5 mg/kg was used to visualise *in vivo* antithrombotic efficacy in the laser-induced endothelium injury model.

Figure 3 (Supplementary movies 3-6) shows the time course of laser-induced thrombus formation and *in vivo* thromboprophylactic efficacy of enoxaparin in the laser-induced endothelium injury model. No thrombus was formed up to 60 min following irradiation using enoxaparin at a dose of 5 mg/kg. To compare laser-induced thrombus size between enoxaparin-pretreated mice and control mice, enoxaparin at a dose of 1 mg/kg was adopted. The mean volumes of laser-induced thrombus 60 min after endothelial injury were 652 ± 432 μm^3 in enoxaparin-pretreated mice (n=5 arterioles from three mice) and 8906 ± 1469 μm^3 in control mice (n=5). Intravenous administration of enoxaparin at a dose of 1 mg/kg significantly inhibited laser-induced thrombus formation ($p < 0.01$),

as compared with control (no-enoxaparin pretreatment).

Thrombolytic effect of enoxaparin in the laser-induced thrombus model in vivo

To visualise the *in vivo* thrombolytic effect, enoxaparin at a dose of 1 mg/kg was administered intravenously 60 min after irradiation of the vascular endothelium. The mean thrombus volume 60 min after laser-induced endothelial injury was 8366 ± 2037 μm^3 (n=3 arterioles from three mice). The mean thrombus volume 60 min after enoxaparin administration was 3643 ± 3384 μm^3 (n=3 arterioles from three mice).

The rates of reduction in thrombus volume by enoxaparin administration were 16.1%, 66.6%, and 94.3 % in each mouse. The mean rate of reduction was 59% ± 39.7%. Intravenous administration of enoxaparin at a dose of 5 mg/kg significantly decreased the size of laser-induced thrombus, as compared with control (no-enoxaparin treatment).

Figure 4 shows an almost complete obstruction 60 min after laser-induced thrombus formation, resulting in a near complete cessation of blood flow. Supplementary movie 7 shows a process of thrombus development with the adhesion of rolling platelets on the surface of the growing thrombus.

Figure 4B shows *in vivo* thrombolytic efficacy of enoxaparin for laser-induced thrombus. Supplementary movie 8 shows a process of thrombolysis with the release of aggregated platelets on the surface of the thrombus at the single platelet level.

Thromboprophylactic efficacy of enoxaparin in the LPS-induced sepsis model in vivo

Postoperative surgical site infection is one of the major concerns among patients undergoing major gastrointestinal surgery because it may develop into lethal sepsis. In general, sepsis causes haemostatic abnormalities and coagulation disorders, resulting in disseminated intravascular coagulation or multiple organ failure/injury. Therefore, we also sought to examine the thromboprophylactic effect of enoxaparin in the LPS-induced sepsis model.

We found that the time to maximum thrombus volume (approximately 8000 μm^3) after laser irradiation was shorter in LPS-administered mice (approximately 30 min after laser-induced endothelium injury) than in control mice (approximately 60 min after injury), indicating hypercoagulation due to LPS.

In the early phase of laser-induced thrombus formation, platelets attached and adhered to the endothelium downstream of the laser-injured region (straight line formation) (**Figure 5A** and Supplementary movie 9). We also observed that enoxaparin pretreatment disturbed straight line formation of platelets in LPS-administered mice, confirming *in vivo* thromboprophylactic efficacy of enoxaparin with LPS-induced sepsis (**Figure 5B** and Supplementary movie 10).

Discussion

The mechanisms underlying platelet aggregation and thrombus formation have been extensively investigated in *in vitro* studies [19, 20]. Animal models (*in vivo* studies) for vascular thrombosis have facilitated our comprehensive understanding of physiological and pathophysiological thrombus formation [21, 22]. Furthermore, intravital imaging of thrombus formation in living animals provides a direct visualisation of the dynamic process of platelet adhesion, aggregation, and thrombus formation in real-time [17, 23, 24].

Previously, we reported a method of *in vivo* real-time imaging of laser-induced thrombus formation using TPLSM with an organ stabilising system, and demonstrated platelet-dependent thrombus development, including platelet translocation, adhesion, aggregation in a linear fashion, and thrombus growth with the adhesion of rolling platelets on the surface of developing thrombus after laser-induced endothelium specific injury [10].

Strengths of our study protocol include clear visualisation of the vascular wall layer at higher magnification and higher resolution because of intravital TPLSM with an organ stabilising system, and sophisticated and reproducible laser irradiation of vascular endothelium owing to clear and nearly static visualisation of vascular layers. In addition, intravascular events, such as platelet-platelet interactions and platelet-endothelial interactions, may be more physiological (or pathophysiological) because there is

no need to label an antibody for platelet visualisation in cellular interactions *in vivo*. Therefore, we believe that our results of thromboprophylactic and thrombolytic efficacy of enoxaparin in an *in vivo* laser-induced vascular endothelial injury model are more reliable and reproducible, compared with those of previously reported procedures [17, 25, 26].

Enoxaparin, one of the LMWHs, has been widely used as an anticoagulant and antithrombotic drug with similar features to heparin *in vitro* and *in vivo*, based on its antithrombin III-activating properties [27, 28].

In this study, we visualised *in vivo* thromboprophylactic and thrombolytic efficacy of enoxaparin at the single platelet level. The thromboprophylactic effect of enoxaparin was strong and constant even at a dose of 1 mg/kg. The thrombolytic effect of enoxaparin was also strong based on the rate of reduction in thrombus size (> 50%). The thromboprophylactic effect of enoxaparin in the LPS-induced sepsis model was also observed. These results complement and support the data regarding thromboprophylactic and thrombolytic effects of enoxaparin previously demonstrated by *in vitro* and *in vivo* studies, and clinical trials.

Several limitations of our study protocol should be taken into account when interpreting our results. Species differences in the efficacy of enoxaparin on thrombogenesis and thrombolysis between humans and mice should be considered. The methods and dosages of enoxaparin administration between our experimental model (intravenous) and clinical use (subcutaneous) are different.

However, intravital TPLSM imaging of thrombus formation at high resolution (at the single platelet level) and high magnification (×600 or higher) is required for further understanding of physiological haemostasis and thrombosis. Our methods may help screen and evaluate new anticoagulant or antiplatelet drugs in preclinical murine thrombosis models.

In conclusion, *in vivo* thromboprophylactic and thrombolytic efficacy of enoxaparin can be visualised at the single platelet level in the laser-induced endothelium injury model using TPLSM. Our methods may help screen and evaluate new anticoagulant or antiplatelet drugs in preclinical murine thrombosis models.

Acknowledgements

This work was partly supported by grants from the Ministry of Education, Culture, Sports, Science and Technology of Japan (KAKENHI 11007576 to K.U., 11020424 to Y.K., and 12011552 to M.K.). This work was also partly supported by the Ichiro Kanehara Foundation. No additional external funding received for this study.

Disclosure of conflict of interest

K.T., A.M. and M.K. designed and performed experiments and analyzed and interpreted data and wrote the manuscript. K.T., Y.K., K.M., and M.O. performed experiments and analyzed data. Y.T., M.K., S.S., Y.O., Y.I., K.U., T.A., and Y.M. designed experiments and analyzed and interpreted data. A.M. and M.K. designed experiments and interpreted data.

Address correspondence to: Koji Tanaka, Department of Gastrointestinal and Paediatric Surgery, Mie University Graduate School of Medicine, 2-174 Edobashi, Tsu, Mie 514-8507, Japan. Tel: +81-59-231-5294; Fax:+81-59-232-6968; E-mail: qouji@clin.medic.mie-u.ac.jp

References

[1] Lee AY, Levine MN. Venous thromboembolism and cancer: risks and outcomes. Circulation 2003; 107: I17-121.

[2] Geerts WH, Heit JA, Clagett GP, Pineo GF, Colwell CW, Anderson FA Jr, Wheeler HB. Prevention of venous thromboembolism. Chest 2001; 119: 132S-175S.

[3] Bergqvist D, Agnelli G, Cohen AT, Eldor A, Nilsson PE, Le Moigne-Amrani A, Dietrich-Neto F; ENOXACAN II Investigators. Duration of prophylaxis against venous thromboembolism with enoxaparin after surgery for cancer. N Engl J Med 2002; 346: 975-980.

[4] Bergqvist D. Low molecular weight heparin for the prevention of venous thromboembolism after abdominal surgery. Br J Surg 2004; 91: 965-974.

[5] Bergqvist D. Risk of venous thromboembolism in patients undergoing cancer surgery and options for thromboprophylaxis. J Surg Oncol 2007; 95: 167-74.

[6] Doutremepuich C, Azougagh Oualane F, Doutremepuich F, Fareed J. New class of heparin derivatives with a potent antithrombotic effect and a very limited hemorrhagic activity. Thromb Res 1996; 83: 217-228.

[7] Fareed J, Jeske W, Eschenfelder V, Iqbal O, Hoppensteadt D, Ahsan A. Preclinical studies on a low molecular weight heparin. Thromb Res 1996; 81: S1-27.

[8] Rebello SS, Kasiewski CJ, Bentley RG, Morgan SR, Chu V, Bostwick JS, Klein SI, Perrone MH, Leadley RJ. Superiority of enoxaparin over heparin in combination with a GPIIb/IIIa receptor antagonist during coronary thrombolysis in dogs. Thromb Res 2001; 102: 261-271.

[9] Toiyama Y, Mizoguchi A, Okugawa Y, Koike Y, Morimoto Y, Araki T, Uchida K, Tanaka K, Nakashima H, Hibi M, Kimura K, Inoue Y, Miki C, Kusunoki M. Intravital imaging of DSS-induced cecal mucosal damage in GFP-transgenic mice using two-photon microscopy. J Gastroenterol 2010; 45: 544-553.

[10] Koike Y, Tanaka K, Okugawa Y, Morimoto Y, Toiyama Y, Uchida K, Miki C, Mizoguchi A, Kusunoki M. In vivo real-time two-photon microscopic imaging of platelet aggregation induced by selective laser irradiation to the endothelium created in the beta-actin-green fluorescent protein transgenic mice. J Thromb Thrombolysis 2011; 32: 138-145.

[11] Morimoto Y, Tanaka K, Toiyama Y, Inoue Y, Araki T, Uchida K, Kimura K, Mizoguchi A, Kusunoki M. Intravital Three-Dimensional Dynamic Pathology of Experimental Colitis in Living Mice Using Two-Photon Laser Scanning Microscopy. J Gastrointest Surg 2011; 15: 1842-1850.

[12] Tanaka K, Morimoto Y, Toiyama Y, Okugawa Y, Inoue Y, Uchida K, Kimura K, Mizoguchi A, Kusunoki M. Intravital dual-colored visualization of colorectal liver metastasis in living mice using two photon laser scanning microscopy. Microsc Res Tech 2012; 75: 307-315.

[13] Tanaka K, Morimoto Y, Toiyama Y, Matsushita K, Kawamura M, Koike Y, Okugawa Y, Inoue Y, Uchida K, Araki T, Mizoguchi A, Kusunoki M. In vivo time-course imaging of tumor angiogenesis in colorectal liver metastases in the same living mice using two-photon laser scanning microscopy. J Oncol 2012; 2012: 265487.

[14] Tanaka K, Toiyama Y, Inoue Y, Uchida K, Araki T, Mohri Y, Mizoguchi A, Kusunoki M. Intravital imaging of gastrointestinal diseases in preclinical models using two-photon laser scanning microscopy. Surg Today 2013; 43: 123-129

[15] Tanaka K, Okigami M, Toiyama Y, Morimoto Y, Matsushita K, Kawamura M, Hashimoto K, Saigusa S, Okugawa Y, Inoue Y, Uchida K, Araki T, Mohri Y, Mizoguchi A, Kusunoki M. In vivo real-time imaging of chemotherapy response on the liver metastatic tumor microenvironment using multiphoton microscopy. Oncol Rep 2012; 28: 1822-1830.

[16] Nishimura N, Schaffer CB, Friedman B, Tsai PS, Lyden PD, Kleinfeld D. Targeted insult to subsurface cortical blood vessels using ultrashort laser pulses: three models of stroke. Nat Methods 2006; 3: 99-108.

[17] Kamocka MM, Mu J, Liu X, Chen N, Zollman A, Sturonas-Brown B, Dunn K, Xu Z, Chen DZ, Alber MS, Rosen ED. Two-photon intravital imaging of thrombus development. J Biomed Opt 2010; 15: 016020.

[18] Okabe M, Ikawa M, Kominami K, Nakanishi T, Nishimune Y. Green mice' as a source of ubiquitous green cells. FEBS Lett 1997; 407: 313-319.

[19] Furie B, Furie BC. Mechanisms of thrombus formation. N Engl J Med 2008; 359: 938-949.

[20] Ruggeri ZM. Platelet adhesion under flow. Microcirculation 2009; 16: 58-83.

[21] Westrick RJ, Winn ME, Eitzman DT. Murine models of vascular thrombosis. Arterioscler Thromb Vasc Biol 2007; 27: 2079-2093.

[22] Sachs UJ, Nieswandt B. In vivo thrombus formation in murine models. Circ Res 2007; 100: 979-991.

[23] Nesbitt WS, Westein E, Tovar-Lopez FJ, Tolouei E, Mitchell A, Fu J, Carberry J, Fouras A, Jackson SP. A shear gradient-dependent platelet aggregation mechanism drives thrombus formation. Nat Med 2009; 15: 665-673.

[24] Takizawa H, Nishimura S, Takayama N, Oda A, Nishikii H, Morita Y, Kakinuma S, Yamazaki S, Okamura S, Tamura N, Goto S, Sawaguchi A, Manabe I, Takatsu K, Nakauchi H, Takaki S, Eto K. Lnk regulates integrin alphaIIbbeta3 outside-in signaling in mouse platelets, leading to stabilization of thrombus development in vivo. J Clin Invest 2010; 120: 179-190.

[25] Dubois C, Panicot-Dubois L, Gainor JF, Furie BC, Furie B. Thrombin-initiated platelet activation in vivo is vWF independent during thrombus formation in a laser injury model. J Clin Invest 2007;117: 953-960.

[26] Rybaltowski M, Suzuki Y, Mogami H, Chlebinska I, Brzoska T, Tanaka A, Banno F, Miyata T, Urano T. In vivo imaging analysis of the interaction between unusually large von Willebrand factor multimers and platelets on the surface of vascular wall. Pflugers Arch 2011; 461: 623-33.

[27] Bourin MC, Lindahl U. Glycosaminoglycans and the regulation of blood coagulation. Biochem J 1993; 289: 313-330.

[28] Weitz JI. Low-molecular-weight heparins. N Engl J Med 1997; 337: 688-98.